Journal of Applied Mechanics and Technical Physics, Vol. 48, No. 2, pp. 176–183, 2007

NUMERICAL SIMULATION OF STABILIZATION OF THE BOUNDARY LAYER ON A SURFACE WITH A POROUS COATING IN A SUPERSONIC SEPARATED FLOW

I. V. Egorov,[1] A. V. Novikov,[2] and A. V. Fedorov[2]

UDC 532.526:533.6.011.5

Stability of a supersonic ($M_\infty = 5.373$) *boundary layer with local separation in a compression corner with a passive porous coating partly absorbing flow perturbations is considered by solving two-dimensional Navier–Stokes equations numerically. The second mode of disturbances of a supersonic boundary layer is demonstrated to be the most important one behind the boundary-layer reattachment point. The possibility of effective stabilization of these disturbances behind the reattachment point with the use of porous coatings is confirmed.*

Key words: *Navier–Stokes equations, supersonic flows, boundary layer, stability, numerical simulation, porous coatings.*

Introduction. In a flow with minor perturbations, the laminar–turbulent transition on an aerodynamically smooth surface occurs because of the growth of various instability modes of the boundary layer. The stability theory and experiments show that the dominating mode in a high-velocity two-dimensional boundary layer is the first or the second mode of disturbances. The first mode corresponds to the Tollmien–Schlichting waves and can be suppressed, for instance, by surface cooling, suction, or favorable pressure gradient [1]. The second mode belongs to a family of acoustic modes predicted theoretically [2] and registered experimentally [3–5]. If the local Mach number is sufficiently high ($M_e > 4$ for a gradientless boundary layer on a thermally insulated surface), the second mode starts dominating, and it is this mode that should be primarily stabilized for flow laminarization. This statement is valid for a flat plate. On a curved surface, disturbances of other types, e.g., essentially three-dimensional Görtler vortices, can also play an important role. In the present paper, however, we do not model three-dimensional disturbances and consider a two-dimensional case.

It was assumed in [6] that the second mode can be stabilized by using a porous coating partly absorbing acoustic disturbances. This hypothesis was confirmed by computations [7] based on the linear stability theory and indirectly validated, in turn, by experiments [8] performed on a sharp cone model in a high-enthalpy wind tunnel at a free-stream Mach number $M_\infty = 5$–6. It was found in these experiments that a coating with uniformly distributed vertical pores in the form of cylindrical blind holes can substantially delay the laminar–turbulent transition.

The experimental studies [9, 10] of stability of the boundary layer on a sharp cone in a T-326 wind tunnel of the Institute of Theoretical and Applied Mechanics of the Siberian Division of the Russian Academy of Sciences at $M_\infty \approx 6$ showed that a porous coating with a random microstructure (metallic felt) suppresses the second mode and exerts an insignificant effect on the first mode. The model in experiments [11] was a cone with a coating having a regular microstructure (perforated thin sheet similar to that used in [8]). This coating was also found to stabilize the second mode and to weakly affect the first mode. The measured phase velocities and amplitudes of disturbances are in reasonable agreement with the linear stability theory.

[1]Joukowski Central Aerohydrodynamic Institute, Moscow Region, Zhukovskii 140180; ivan_egorov@falt.ru. [2]Moscow Institute of Physics and Technology, Moscow Region, Zhukovskii 140180; AndrewNovikov@yandex.ru; fedorov@falt.ru. Translated from Prikladnaya Mekhanika i Tekhnicheskaya Fizika, Vol. 48, No. 2, pp. 39–47, March–April, 2007. Original article submitted February 7, 2006; revision submitted May 15, 2006.

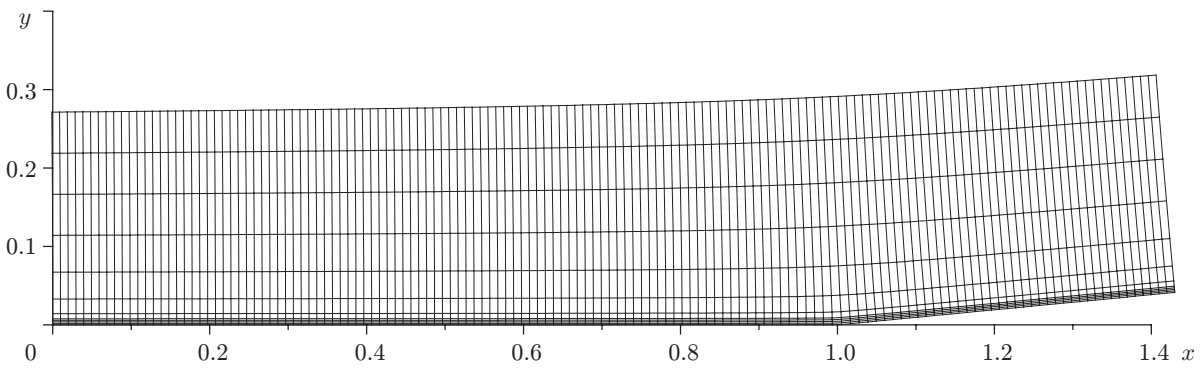

Fig. 1. Computational domain and grid used in the problem (compression angle $\alpha = 5.5^\circ$).

In the above-cited papers, the stability was computed either in the locally parallel approximation or with partial allowance for nonparallelism effects; viscous-inviscid interaction and nonlinear effects were ignored. Interaction of external disturbances (acoustic, vortex, and entropy disturbances) of the incoming flow with the porous coating was not simulated either. To take these factors into account, one has to perform direct numerical simulations by methods developed in [12–14] for problems of stability of high-velocity near-wall flows. Note that the method of direct numerical simulation enables one to estimate the efficiency of the porous coating in strongly nonuniform flows, such as the flows in regions of boundary-layer separation and reattachment, where the classical stability theory is inapplicable.

In the present work, we used a total variation diminishing (TVD) scheme of the second order of approximation in space and time to numerically solve the Navier–Stokes equations for unsteady two-dimensional compressible flows. Stability of a supersonic boundary layer with local separation in a compression corner at a free-stream Mach number $\mathrm{M}_\infty = 5.373$ was considered. The computations were performed for two-dimensional disturbances developed on a solid surface and on a porous coating with a regular microstructure and different pore sizes.

Formulation of the Problem and Numerical Method. The Navier–Stokes equations for two-dimensional viscous compressible unsteady flows are solved. In dimensionless form, the system of equations is given, for instance, in [13]. The dependent variables are normalized to the corresponding free-stream parameters: the pressure is normalized to the doubled dynamic pressure $\rho^*_\infty (U^*_\infty)^2$ (ρ^*_∞ and U^*_∞ are the free-stream density and velocity, respectively); the coordinates are normalized to the reference length L^*, which is the distance from the leading edge of the plate to the inflection point (Fig. 1); the time is normalized to L^*/U^*_∞. The following similarity parameters are used: the Reynolds number $\mathrm{Re}_\infty = L^* U^*_\infty \rho^*_\infty / \mu^*_\infty$, the free-stream Mach number M_∞, the ratio of specific heats of a perfect gas γ, and the Prandtl number Pr; the asterisk indicates dimensional quantities, and the subscript ∞ refers to free-stream parameters. The results discussed below were obtained at $\mathrm{M}_\infty = 5.373$, $\mathrm{Re}_\infty = 5.667 \cdot 10^6$, $\gamma = 1.4$, $\mathrm{Pr} = 0.72$, and $T^*_\infty = 74.194$ K. The dynamic viscosity μ was calculated by Sutherland's formula $\mu = T^{3/2}(T_\mu + 1)/(T_\mu + T)$, where $T^*_\mu = 110$ K.

To solve the problem numerically, we used an implicit finite-volume method with the second order of approximation in space and time. We used a quasi-monotonic Godunov-type scheme (TVD scheme), which is most efficient if the computational domain contains shock waves and other strong spatial inhomogeneities of the flow, such as boundary-layer separation. The previous computations of an unsteady field of disturbances on a flat plate with a sharp leading edge [13] showed that this scheme may be used for problems of stability of a supersonic boundary layer.

Figure 1 shows the computational domain of the problem. The boundary conditions were the no-slip conditions on the lower boundary of the domain (zero vertical and horizontal components of velocity: $u = v = 0$), the free-stream conditions on the left and upper boundaries, and linear extrapolation of the dependent variables u, v, p, and T on the right boundary ("soft" boundary conditions). The plate surface was assumed to be isothermal and to have a temperature $T^*_w = 300$ K ($T_w = 4.043$). The computations were performed on a curved orthogonal grid with 2801×221 nodes (Fig. 1 shows each 20th line) obtained by conformal mapping of the upper half-plane onto the computational domain:

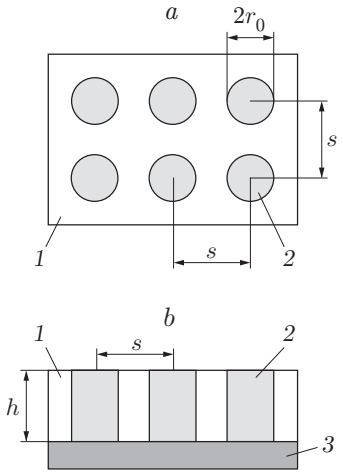

Fig. 2. Porous layer: top view (a) and side view (b); 1) perforated sheet; 2) pores; 3) solid substrate.

$$x = -(\xi^2 + \eta^2)^{(1-\varphi)/2} \cos\left((1-\varphi)\arctan\,(\xi,\eta)\right) + 1,$$
$$y = (\xi^2 + \eta^2)^{(1-\varphi)/2} \sin\left((1-\varphi)\arctan\,(\xi,\eta)\right),$$
$$\varphi = \alpha/\pi.$$

The grid was refined near the surface, so that 55% of the nodes were within the boundary layer and the separation region with the mixing layer.

The problem was solved in three stages. A steady flow field was first computed by a time-dependent method. Then unsteady disturbances were imposed onto the steady solution to study boundary-layer stability: local periodic injection-suction was introduced on the wall. This factor was simulated by a nonuniform boundary condition imposed onto the mass-flow perturbation:

$$q_w(x,t) = \frac{\rho_w^* v_w^*}{\rho_\infty^* U_\infty^*} = \varepsilon \sin\left(2\pi\,\frac{x - x_1}{x_2 - x_1}\right) \sin(\omega t), \qquad x_1 \leqslant x \leqslant x_2.$$

Here $x = x^*/L^*$ is the dimensionless longitudinal coordinate, $x_1 = 0.0358$ and $x_2 = 0.0521$ are the boundaries of the injection-suction region, and $\omega = \omega^* L^*/U_\infty^* = 450$ is the dimensionless frequency corresponding to the frequency parameter $F = \omega/\mathrm{Re}_\infty = 7.94 \cdot 10^{-5}$; the subscript w refers to conditions on the wall (surface). To provide a linear regime of evolution of disturbances before separation and, hence, to make comparisons with the linear theory possible, we chose a rather low forcing amplitude $\varepsilon = 10^{-3}$. The unsteady problem was computed until a periodic field of disturbances was established ($t \approx 1.75$).

At the third stage of computations, boundary conditions simulating interaction of disturbances with a porous layer on an inclined surface (downstream from the inflection point) were introduced into the procedure of solving the unsteady problem to study the effect of the porous coating. The computation was continued from the time $t \approx 1.75$ until a periodic field of disturbances was established again ($t \approx 2.25$). The porous wall ($x > 1.0$) was subjected to an unsteady boundary condition in accordance with the theoretical model developed in [15] and extended in [7] to the second-mode disturbances. After the transition from the complex quantities used in [7] to real quantities, the boundary condition acquires the form

$$u_w(x,t) = -V_w^n(x,t)\sin\alpha, \qquad v_w(x,t) = V_w^n(x,t)\cos\alpha,$$

$$V_w^n(x,t) = p'_w(x,t)\,\mathrm{Real}\,(A) - \frac{1}{\omega}\,\frac{\partial p'_w(x,t)}{\partial t}\,\mathrm{Imag}\,(A),$$

where $V_w^n(x,t)$ is the velocity component normal to the wall, $p'_w(x,t) = p_w(x,t) - p_w(x,0)$ is the pressure perturbation on the wall (difference between the instantaneous value of pressure and the pressure corresponding to the solution of the steady problem prior to introduction of disturbances), $A = \phi \tanh(\Lambda h)/Z_0$ is the permeability of

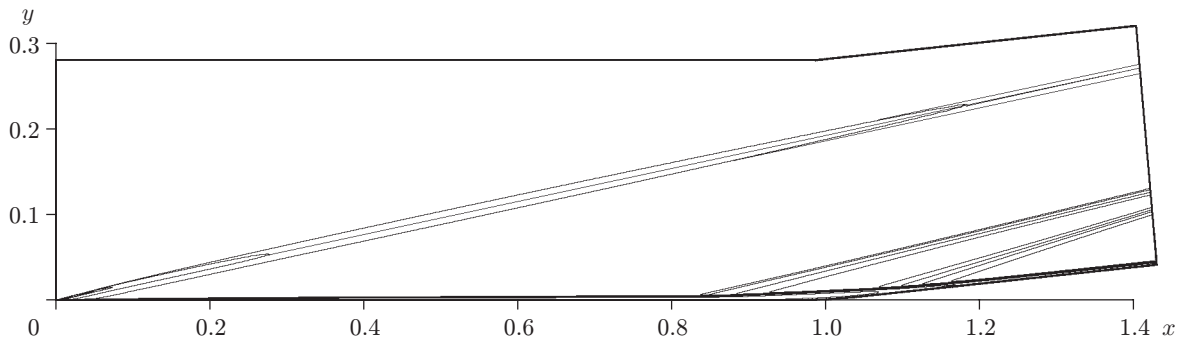

Fig. 3. Density contours of a steady flow field.

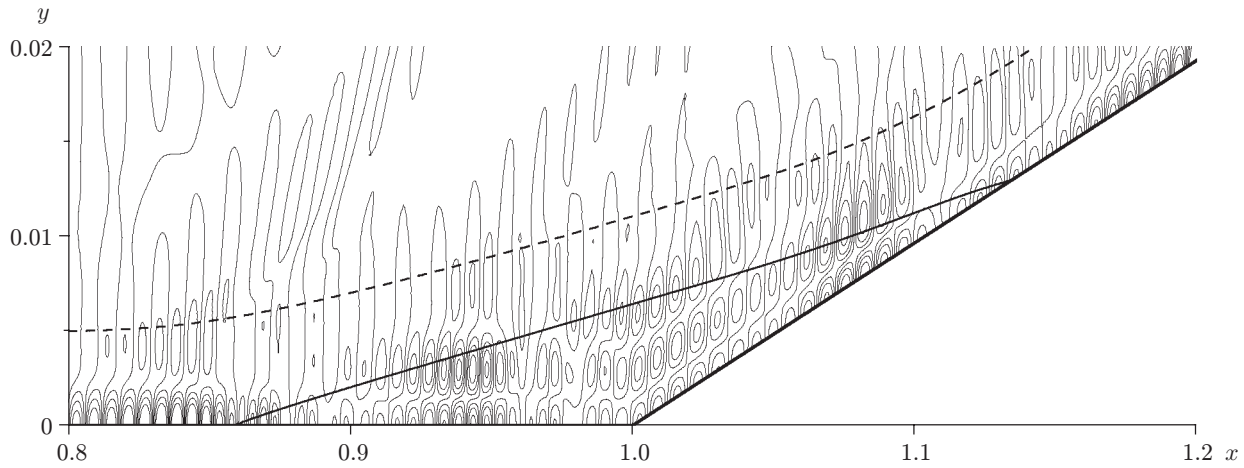

Fig. 4. Contours of pressure perturbations in the separation region for problems with a solid wall and a porous wall: the dashed curve shows the boundary of the mixing layer; the solid curve is the zero streamline.

the porous layer [15], ϕ is the porosity (ratio of the volume of pores to the total volume of the porous layer), and Z_0 and Λ are the characteristic impedance and the propagation constant for an individual pore.

In the computations, we used a coating model with uniformly distributed vertical cylindrical blind holes (pores). The porous layer is schematically shown in Fig. 2 (the dimensionless radius of the pore is $r_0 = 1.5 \cdot 10^{-4}$ and the layer thickness is $h = 10r_0 = 1.5 \cdot 10^{-3}$). For such a coating, the values of Z_0 and Λ are calculated by the algorithm described in [7].

Computation Results. Figure 3 shows the computed steady density field. Viscous-inviscid interaction is responsible for formation of a shock wave in the vicinity of the leading edge. Further downstream, the compression corner induces an oblique shock whose interaction with the boundary layer in the vicinity of the corner point leads to formation of a recirculation zone. The upper boundary of the separation region is an almost straight line, which is typical of supersonic flows. Two compression waves are formed in the vicinity of the separation and reattachment points. The resultant steady field is in good agreement with the results of [14], where the same flow regime was computed by a WENO scheme of the fifth-order accuracy of space discretization.

Figure 4 shows the field of pressure perturbations in the separation region. In these computations and in what follows, this field is obtained by subtracting the initial steady field from the instantaneous unsteady field. Forced oscillations induced by the vibrator are seen on the surface upstream of the separation point. Fast acoustic waves emitted by the injection-suction source are visible above the boundary layer and the mixing layer. Acoustic disturbances generated in the vicinity of the inflection point are manifested in the separation region in the form of vertically aligned cellular structures.

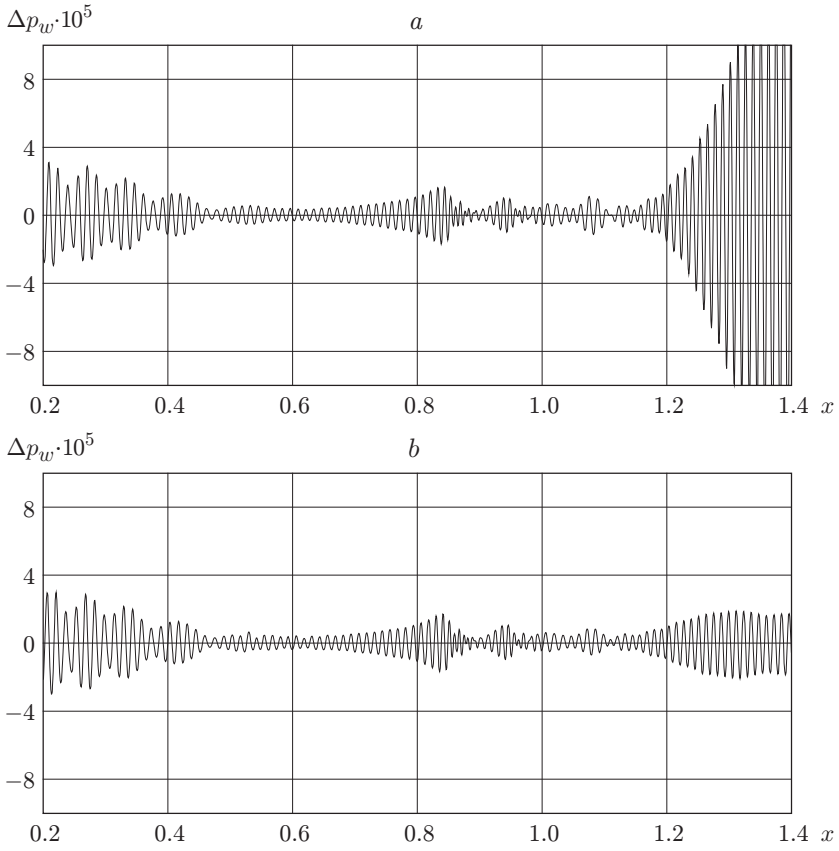

Fig. 5. Pressure fluctuations on the surface: (a) solid wall; (b) porous wall with $x > 1$ and $\phi = \pi/16$.

The computations for a porous surface were performed for $\phi = \pi/9$ and $\pi/16$ corresponding to the distances between the centers of the neighboring pores $s = 3r_0$ and $4r_0$. The parameters were chosen to have approximately 20 pores in the streamwise direction in a segment equal to the length of the second-mode wave ($\lambda \approx 0.012$ for a disturbance frequency $\omega = 450$). For such a high concentration of pores and their small radius, the coating roughness seems to be negligibly small, but the porous layer can efficiently absorb perturbations penetrating into the layer [6, 7, 11].

The simulated structure of the field of disturbances in the problem with a porous surface is similar to the structure of disturbances in the problem with a solid surface (only the disturbance amplitudes are different); therefore, in particular, Fig. 4 is valid for both problems. For interpreting the effect of the porous coating, this property allows one to consider fluctuations on the surface only. Figure 5 shows the distributions of pressure perturbations on a solid wall and on a porous surface. At the exit from the computational domain, the porous coating leads to an approximately ninefold decrease in the disturbance amplitude ($\phi = \pi/16$). This effect is even more pronounced for porosity $\phi = \pi/9$: the amplitude decreases by a factor of 12. In the region $1.0 < x < 1.2$ (up to the point of reattachment $x \approx 1.136$), the amplitudes on the porous and solid surfaces are almost identical.

It seems of interest to consider which type of disturbances is most strongly affected by the porous coating. Based on the distribution of fluctuations on the surface (see Fig. 5), we found a discrete set of local wavelengths of disturbances $\lambda(x_c) = x_{\max 2} - x_{\max 1}$, where $x_{\max 1}$ and $x_{\max 2}$ are the coordinates of the neighboring maximums on the plot; $x_c = (x_{\max 1} + x_{\max 2})/2$. After that, continuous dependences of the wavenumber and phase velocity on the x coordinate were obtained with the use of a five-point smoothing filter on the basis of the fast Fourier transform: $k(x) = 2\pi/\lambda(x)$ and $c(x) = \omega/k(x)$ (Fig. 6). (The vertical lines in Fig. 6 are drawn through the points of separation, inflection, and reattachment.) The disturbances approach the separation point with a phase velocity $c = 0.9$, and exponential growth of the amplitude is observed at this point (see Fig. 5). A comparison with the

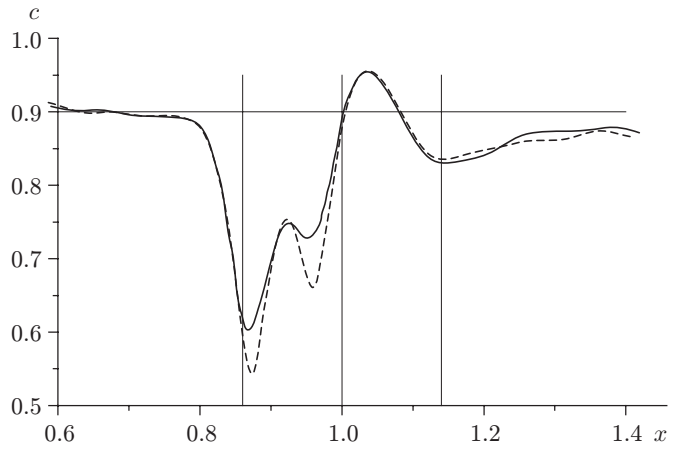

Fig. 6. Phase velocity of the wave of disturbances: the solid and dashed curves refer to the solid and porous walls, respectively.

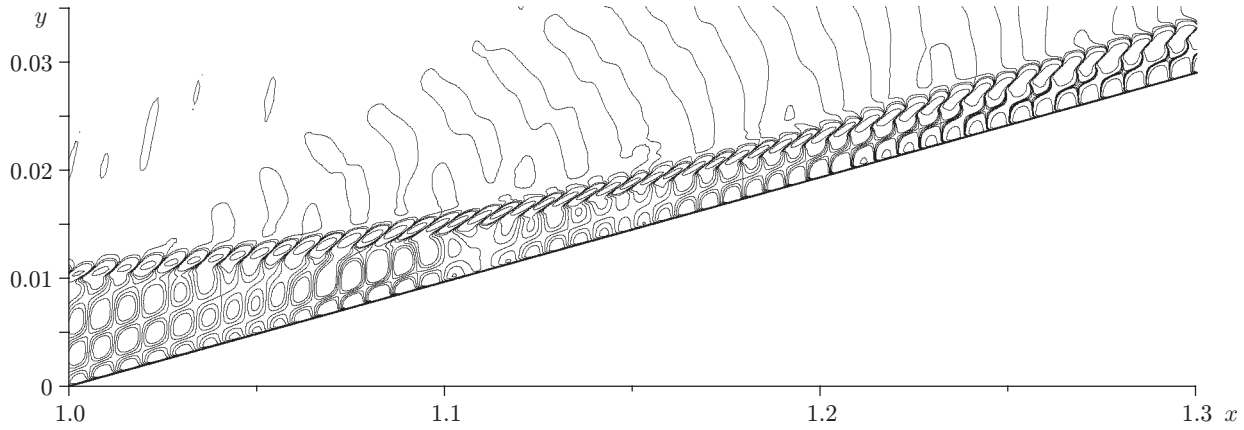

Fig. 7. Contours of temperature disturbances near the reattachment point.

linear theory applicable upstream of the separation, as in the case of a flat plate, which was performed in [13], showed that this growth corresponds to the second mode with a characteristic phase velocity $c = 0.9$. Behind the reattachment point, the phase velocity of disturbances again approaches a value of 0.9, and exponential growth of the amplitude is observed, which may be caused by second-mode instability, as in the flat-plate case. This is confirmed by topology of the field of temperature fluctuations in the boundary layer, which is shown in Fig. 7 (such a pattern is observed on both the porous and the solid wall). The spindle structure typical of the second model of disturbances is clearly seen. Thus, in the problem considered, the second-mode disturbances dominate, which are efficiently stabilized by a porous coating.

It should be noted that the phase velocity of the wave in the separation region (see Fig. 6) is far from the value $c = 0.9$. There is also a difference in phase velocities for the porous and solid walls, because the curves in Fig. 6 were computed for different times. This behavior of the phase velocity, which is caused apparently by the presence of the traveling wave, and the results of an analysis of disturbances in Fig. 4 allow us to argue that long-wave (propagating in the transverse direction) acoustic disturbances prevail in the separation region; the reason for these disturbances seems to be secondary reflections of forced perturbations from the inflection. Note that these acoustic disturbances remain almost unaffected by the porous coating (see Fig. 5), i.e., there are no side effects, which could, for instance, amplify acoustic disturbances in the separation region.

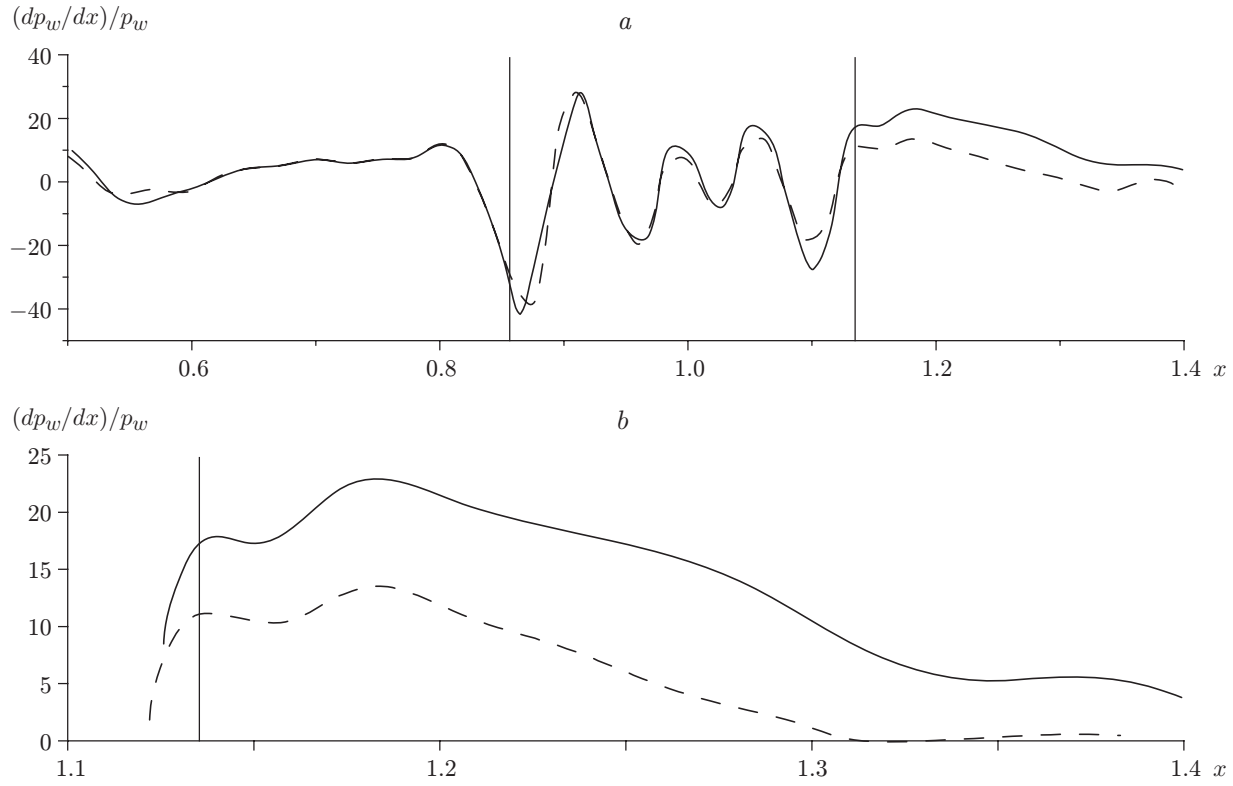

Fig. 8. Growth rate of the amplitude of fluctuations on the solid surface (solid curves) and on a porous surface with $\phi = \pi/16$ (dashed curves): (a) full scale in the x direction; (b) region behind the reattachment point in the zone of growth of the second mode of disturbances.

The effect of the porous coating on the growth rate of disturbances $\sigma = d[\ln p'_w(x)]/dx$ is plotted in Fig. 8 (the vertical lines are drawn through the points of separation and reattachment). The effect of stabilization is not well seen in the full-scale figure (Fig. 8a) because of the large fluctuations of the growth rate in the separation region, but the magnified picture of the region of interest behind the reattachment point (Fig. 8b) clearly shows that the porous coating reduces the growth rate of disturbances more than twofold. As it could be expected, the growth rates upstream of the reattachment point are identical for the solid and porous walls (Fig. 8a).

Conclusions. Stability of a supersonic boundary layer in a compression corner with a solid surface and with a surface covered by a porous layer is simulated by means of numerical integration of two-dimensional Navier–Stokes equations. For this purpose, perturbations of the injection-suction type, local in space and harmonic in time, are introduced into the boundary layer. The model of a coating with equidistant cylindrical blind pores is demonstrated to substantially reduce the growth rate of the second mode. In particular, for a porosity approximately equal to 20%, the amplitude of the second mode at the output boundary of the computational domain decreases by a factor of 9.

It should be noted that the porous layer weakly affects the acoustic component of disturbances in the boundary layer, i.e., the porous coating does not produce adverse effects of secondary reflections of acoustic waves in the separation region. Such effects could lead to resonant amplification of disturbances and, as a consequence, to an early transition in the boundary layer. Yet, the question of the roughness of the porous surface, which exists in reality and is not simulated in this work, remains open. In addition, edge effects on the pore are ignored in [7] in deriving the boundary conditions for a porous coating. Finally, the present computations ignore three-dimensional disturbances, such as the Görtler vortices, which may exert a significant effect on the examined phenomenon. All these phenomena require further investigations.

The numerical simulations performed support the concept of stabilization of boundary-layer perturbations with the use of a passive porous coating at sufficiently high free-stream Mach numbers.

This work was supported by the Russian Foundation for Basic Research (Grant No. 06-08-01214).

REFERENCES

1. S. A. Gaponov and A. A. Maslov, *Development of Disturbances in Compressible Flows* [in Russian], Nauka, Novosibirsk (1980).
2. L. M. Mack, "Boundary layer stability theory," Doc. No. 900-277, Rev. A, Jet Propulsion Laboratory, Pasadena (1969).
3. J. M. Kendall, "Wind tunnel experiments relating to supersonic and hypersonic boundary layer transition," *AIAA J.*, **13**, 290–299 (1975).
4. A. Demetriades, "Hypersonic viscous flow over a slender cone. Part 3. Laminar instability and transition," AIAA Paper No. 74-535 (1974).
5. K. F. Stetson, E. R. Thompson, J. C. Donaldson, and L. G. Siler, "Laminar boundary layer stability experiments on a cone at Mach 8. Part 1. Sharp cone," AIAA Paper No. 83-1761 (1983).
6. N. D. Malmuth, A. V. Fedorov, V. I. Shalaev, et al., "Problems in high speed flow prediction relevant to control," AIAA Paper No. 98-2695 (1998).
7. A. V. Fedorov, N. D. Malmuth, A. Rasheed, and H. G. Hornung, "Stabilization of hypersonic boundary layers by porous coatings," *AIAA J.*, **39**, No. 4, 605–610 (2001).
8. A. Rasheed, H. G. Hornung, A. V. Fedorov, and N. D. Malmuth, "Experiments on passive hypervelocity boundary layer control using a ultrasonically absorptive surface," *AIAA J.*, **40**, No. 3, 481–489 (2002).
9. V. M. Fomin, A. V. Fedorov, A. N. Shiplyuk, et al., "Stabilization of a hypersonic boundary layer by coatings absorbing ultrasound," *Dokl. Ross. Akad. Nauk*, **384**, No. 2, 1–5 (2002).
10. A. Fedorov, A. Shiplyuk, A. Maslov, et al., "Stabilization of a hypersonic boundary layer using an ultrasonically absorptive coating," *J. Fluid Mech.*, **479**, 99–124 (2003).
11. A. Fedorov, V. Kozlov, A. Shiplyuk, et al., "Stability of hypersonic boundary layer on porous wall with regular microstructure," AIAA Paper No. 2003-4147 (2003).
12. X. Zhong, "Leading-edge receptivity to free-stream disturbance waves for hypersonic flow over parabola," *J. Fluid Mech.*, **441**, 315–367 (2001).
13. I. V. Egorov, V. G. Sudakov, and A. V. Fedorov, "Numerical simulation of propagation of disturbances in a supersonic boundary layer," *Izv. Ross. Akad. Nauk, Mekh. Zhidk. Gaza*, No. 6, 33–44 (2004).
14. P. Balakumar, H. Zhao, and H. Atkins, "Stability of hypersonic boundary-layers over a compression corner," AIAA Paper No. 2002-2848 (2002).
15. S. A. Gaponov, "Effect of gas compressibility on the stability of a boundary layer above a permeable surface at subsonic velocities," *J. Appl. Mech. Tech. Phys.*, 16, No. 1, 95–98 (1975).